Redox Biology 53 (2022) 102345

Contents lists available at ScienceDirect

Redox Biology

journal homepage: www.elsevier.com/locate/redox

Rhodaneses minimize the accumulation of cellular sulfane sulfur to avoid disulfide stress during sulfide oxidation in bacteria

Mingxue Ran [a], Qingbin Li [a], Yufeng Xin [c], Shaohua Ma [a], Rui Zhao [a], Min Wang [a], Luying Xun [a,b,**], Yongzhen Xia [a,*]

[a] State Key Laboratory of Microbial Technology, Shandong University, Qingdao, 266237, People's Republic of China
[b] School of Molecular Biosciences, Washington State University, Pullman, WA, 99164-7520, USA
[c] College of Life Sciences, Qufu Normal University, Qufu, 273165, China

ARTICLE INFO

Keywords:
Sulfide oxidation
Sulfide: quinone oxidoreductase
Persulfide dioxygenase
Rhodanese
Sulfane sulfur
Glutathione persulfide

ABSTRACT

Heterotrophic bacteria and human mitochondria often use sulfide: quinone oxidoreductase (SQR) and persulfide dioxygenase (PDO) to oxidize sulfide to sulfite and thiosulfate. Bioinformatic analysis showed that the genes encoding RHOD domains were widely presented in annotated *sqr-pdo* operons and grouped into three types: fused with an SQR domain, fused with a PDO domain, and dissociated proteins. Biochemical evidence suggests that RHODs facilitate the formation of thiosulfate and promote the reaction between inorganic polysulfide and glutathione to produce glutathione polysulfide. However, the physiological roles of RHODs during sulfide oxidation by SQR and PDO could only be tested in an RHOD-free host. To test this, 8 genes encoding RHOD domains in *Escherichia coli* MG1655 were deleted to produce *E. coli* RHOD-8K. The sqr_{Cp} and pdo_{Cp} genes from *Cupriavidus pinatubonensis* JMP134 were cloned into *E. coli* RHOD-8K. SQR_{Cp} contains a fused RHOD domain at the N-terminus. When the fused RHOD domain of SQR_{Cp} was inactivated, the cells oxidized sulfide into increased thiosulfate with the accumulation of cellular sulfane sulfur in comparison with cells containing the intact sqr_{Cp} and pdo_{Cp}. The complementation of dissociated DUF442 minimized the accumulation of cellular sulfane sulfur and reduced the production of thiosulfate. Further analysis showed that the fused DUF442 domain modulated the activity of SQR_{Cp} and prevented it from directly passing the produced sulfane sulfur to GSH. Whereas, the dissociated DUF442 enhanced the PDO_{Cp} activity by several folds. Both DUF442 forms minimized the accumulation of cellular sulfane sulfur, which spontaneously reacted with GSH to produce GSSG, causing disulfide stress during sulfide oxidation. Thus, RHODs may play multiple roles during sulfide oxidation.

1. Introduction

H_2S is the most versatile molecule for early life on Earth [1]. Recently, its physiological and signaling roles in plants, animals, and microorganisms have attracted attention [2–5]. However, excess sulfide is toxic to cells [6]. It inhibits cellular respiration by poisoning cytochrome *c* oxidase or raises oxidative stress with reactive sulfur species [7,8]. We have recently reported that most heterotrophic bacteria are actively producing H_2S during growth, and many of them can oxidize self-produced H_2S by using sulfide: quinone oxidoreductases (SQR) [9] or flavocytochrome c-sulfide dehydrogenases (FCSDs) [10]. SQR, which is more active for sulfide oxidation than FCSDs, often forms an operon with persulfide dioxygenase (PDO) in bacterial phylum [9,11]. Sulfide oxidation by SQR and PDO has been reported in human mitochondria, *Staphylococcus aureus,* and *Cupriavidus pinatubonensis* JMP134 as a function of H_2S detoxification [12–16]. SQR oxidizes H_2S to sulfane sulfur (S^0). PDO oxidizes S^0 in the form of organic persulfide (e.g., GSSH, CoASSH, and BSSH) to sulfite. Sulfite reacts with S^0 to form thiosulfate either spontaneously or with the help of RHODs [11,15].

In bacteria, the *sqr* and *pdo* genes are often next to each other to form operons on the chromosome (*9*). Further, rhodanese (RHOD, EC 2.8.1.1) genes are often clustered with *sqr* and *pdo* genes with some being even fused with SQR or PDO [8,11,14]. RHODs are also ubiquitous in all three domains of life [17]. They exist as single-domain proteins, such as human TSTD1 [12] and *E. coli* GlpE [18], or as multiple domain proteins, such as bovine RHOD Rhobov [19] and *Azotobacter vinelandii*

* Corresponding author. 72 Binhai Road, Qingdao 266237, People's Republic of China.
** Corresponding author. School of Molecular Biosciences, Washington State University, Pullman, WA, 991647520, USA.
E-mail addresses: luying_xun@vetmed.edu.edu (L. Xun), xiayongzhen2002@sdu.edu.cn (Y. Xia).

https://doi.org/10.1016/j.redox.2022.102345
Received 20 March 2022; Received in revised form 4 May 2022; Accepted 16 May 2022
Available online 26 May 2022

RHOD RhdA [20]. They are also present as fusions with other protein domains [21,22].

RHODs catalyze via a ping-pong mechanism, with an active site cysteine residue carrying the transferred sulfur as a covalent intermediate. The catalytic cysteine is the first residue of a loop of six amino acid residues that folds in a cradle-like structure [17,23]. The sulfane sulfur in thiosulfate, polysulfide [11], and GSSH [13] serves as the sulfur donor, and the sulfane acceptors are compounds that can receive sulfane sulfur, such as cyanide, GSH [13], sulfite [12], and thioredoxin [18,24]. Therefore, RHODs transfer sulfane sulfur among various acceptors, maintaining a sulfane sulfur pool in the cytoplasm ([25,26]). RHODs participate in selenium metabolism [27] and the syntheses of Fe–S cluster [23], thiamin [22], and molybdenum cofactor [28,29]. RHODs may also contribute to redox homeostasis, but the intrinsic mechanism is unknown [30–33].

RHODs play various roles during sulfur oxidation by SQR and PDO. TSTD1 is the functional RHODs in the SQR-PDO pathway in human cells, and it catalyzes the transfer of sulfane sulfur from GSSH to sulfite, producing GSH and thiosulfate [13]. An RHOD domain fused to the C-terminus of persulfide dioxygenase (CstB) from *S. aureus* promotes thiosulfate formation during sulfide oxidation [15]. Reversely, the RHOD domain of a PDO-RHOD fusion from *Burkholderia phytofirmans* transfers sulfur from thiosulfate to GSH, producing GSSH, which is oxidized by PDO to sulfite [34]. CstA is an RHOD-TusA-TusD fusion, in *S. aureus*, and the RHOD domain can transfer sulfur from thiosulfate to TusA and TusD Cys thiols, which may pass the sulfane sulfur to other potential receptors [14]. Most of these studies mainly focus on the activity of RHOD at a biochemical level.

We recently reported that a DUF442 domain fused at the N-terminus of SQR (fDUF442) from *C. pinatubonensis* JMP134 is also an RHOD domain [11]. Although the recombinant dissociatively expressed DUF442 domain (dDUF442) accelerates the reaction of GSH with inorganic polysulfide (H_2S_n, $n > 2$) to produce GSSH as well as the reaction of GSSH with sulfite to produce thiosulfate, the inactivation of fDUF442 in SQR did not demonstrate whether RHOD enhanced thiosulfate production by a recombinant *Escherichia coli* carrying SQR_{Cp} and PDO_{Cp} from *C. pinatubonensis* JMP134. Since *E. coli* strain K-12 displays robust RHOD activity and encodes 9 proteins with RHOD domain [35], the effect of DUF442 could be compensated by the host RHODs.

Here we found the RHOD domains were widely distributed in an *sqr-pdo* operon and could be categorized into three types: fused with an SQR domain, fused with a PDO domain, and dissociated proteins. To identify the functions of these RHOD domains, the sqr_{Cp}, and pdo_{Cp} genes were cloned into an *E. coli* mutant without RHOD activities. The inactivation of the RHOD activity of fDUF442 resulted in the accumulation of cellular sulfane sulfur and increased production of thiosulfate, and the changes were minimized by providing dissociated DUF442 (dDUF442). Both prevented sulfane sulfur accumulation but via different mechanisms: fDUF442 modulated the SQR activity, and dDUF442 stimulated the PDO activity. The accumulation of cellular sulfane sulfur causes disulfide stress. These results reveal an important function of RHODs in minimizing cellular sulfane sulfur accumulation.

2. Materials and methods

2.1. Bacterial strains and culture conditions

Bacterial strains used in this study are listed in Table S1. *E. coli* strains were cultured in lysogeny broth (LB) at 37 °C or 30 °C, as indicated. *C. pinatubonensis* JMP134 was cultured in LB medium at 30 °C. Kanamycin (50 μg/mL), spectinomycin (50 μg/mL) or ampicillin (100 μg/mL) were added when required.

2.2. General DNA manipulations

Plasmids used in this study are listed in Table S1. Synthetic primers with characteristics and purposes are listed in Table S2. Bacterial genomes were purified with the TIANamp Bacterial DNA kit (TIANGEN, China). Plasmids were extracted with the E.Z.N.A Plasmid Mini kit (Omega, USA). Phusion DNA polymerase (Thermo, USA) was used for DNA amplification according to the recommended instructions. Cloning was conducted by using the simple TEDA method [36]. Sequence editing for cloned genes was achieved by using an optimized QuikChange method [46].

Gene deletion mutants of *E. coli* MG1655 were constructed by using a reported one-step deletion method [37], with long homology arms to enhance the success rate [38]. Nine genes encoding RHOD domains were deleted in a defined order (Fig. S1).

Genes encoding PDO_{Cp} (WP_041680387.1), SQR_{Cp} (WP_011299713.1), and the DUF442 domain of SQR_{Cp} (dDUF442) were ensembled into pET-30 Ek/LIC plasmid under the control of T7 promoter or pBBR1MCS2 and pCL1920 under the control of the Plac promoter by using the TEDA method. To test the RHOD activity, nine genes encoding the RHOD domain from *E. coli* were cloned into pCL1920 (*36*). To change the ratios of SQR_{Cp} to PDO_{Cp} in recombinant *E. coli* strains, the ribosome binding sequences (RBSs) of the two genes were modified in pMCS2:ppdo_{Cp}-nsqr_{Cp} (Fig. S2). First, the RBS for PDO_{Cp} was changed to its native sequence, and then the nRBS sequence for SQR_{Cp} was changed into BBa_B0031 (a1RBS), BBa_B0032 (a2RBS), and BBa_B0033 (a3RBS), which are listed in the iGEM website (http://parts.igem.org/Main_Page). The fDUF442 domain was inactivated by site-directed mutagenesis, changing Cys94 to Ser94. His-Tag was added to the C-terminal of PDO_{Cp}, SQR_{Cp}, and dDUF442 for purification and western blot detection.

2.3. Resting cells preparation

E. coli strains with cloned genes were cultured in LB medium at 37 °C until OD_{600} reached 0.6. Isopropyl β-D-Thiogalactoside (IPTG) was added at a final concentration of 0.4 mM, and the cells were further cultured at 30 °C for 4 h. The cells were harvested by centrifugation at 3000×*g* for 10 min, resuspended in 50 mM Tris-HCl buffer (pH 7.4) with 50 μM diethylenetriamine pentaacetic acid (DTPA), and collected by centrifugation again. The washed cell pellets were resuspended in the same buffer at OD_{600} of 2 and stored on ice before whole-cell assays.

2.4. SQR-containing membrane preparation

E. coli BL21 (DE3) cells with pET:sqr_{Cp} or pET:sqr_{Cp}-C94S were cultured in 100 mL of LB medium at 37 °C until OD_{600} reached 0.6. The cultures were induced with 0.4 mM IPTG and cultivated at 30 °C for 12 h. Cells were harvested and washed by centrifugation, and the washed cells were resuspended in 10 mL of 50 mM Tris-HCl (pH = 7.4). The resuspended cells were disrupted with a pressure cell homogenizer (Model SPCH-18, Stansted Fluid Power LTD, Harlow, UK) at 4 °C. The lysate was centrifuged at 12000×*g* for 10 min to remove cell debris. The supernatant was ultra-centrifuged at 270000×*g* for 60 min to obtain membrane fractions. The membrane fractions were resuspended in 50 mM Tris-HCl (pH = 7.4) buffer, and then 50% glycerol was added to a final concentration of 10% before the preparation was stored at −80 °C. The protein concentration of the membrane fraction was determined by using the BCA method (Beyotime, China). The crude membrane fraction with SQR_{Cp} was used to assay SQR activity.

2.5. The protein purification of PDO_{Cp} and dDUF442

E. coli BL21 (DE3) cells harboring plasmids pET:pdo_{Cp} or pET:$duf442_{Cp}$ were cultured, induced, harvested, washed, and disrupted as described in the previous section, except that the cells were disrupted in buffer I (20 mM Tris-HCl, 0.3 M NaCl, 20 mM imidazole, pH 8.0). Cell debris was removed by using centrifugation at 12500×*g* for 10 min. Target proteins were purified by using nickel-nitrilotriacetate (Ni-NTA)

agarose (Qiagen, Shanghai, China), according to the supplier's recommendation. The final buffer was exchanged to 50 mM Tris-HCl (pH = 7.4) buffer by using PD-10 desalting column (GE Healthcare), and then 50% glycerol was added to a final concentration of 10% before storing at −80 °C. The protein concentration was estimated by using the BCA method (Beyotime, China). The purified PDO_{Cp} was used to assay PDO activity.

2.6. RHOD activity assays

The RHOD activity was assayed according to a reported method [39]. Briefly, RHOD was added into 50 mM thiosulfate and 50 mM cyanide in 1 mL of 50 mM Tris buffer (pH 7.4) to initiate the reaction at 25 °C for 5 min. Then, 250 μL of 37% formaldehyde was added to stop the reaction, and then 100 μL of the ferric nitrate reagent was added for color formation. After 10 min, the mixture was centrifuged to remove the precipitate, and $Fe(SCN)_3$ in the supernatant was determined at A_{460}. For cell extracts assays, the resting cells disrupted in the Tris buffer at OD_{600} = 2 were used. The activity detection for purified dDUF442 or the membrane fraction with SQR_{Cp}, a defined amount of proteins as indicated in the text was added into the Tris buffer to start the reaction. The memebrane fractions with SQR_{Cp} were used to represent fDUF442. One unit (U) of RHOD activity was defined to form 1 nmol SCN^- per 1 min. The specific activity was expressed as U per mg of protein (nmol min^{-1} mg^{-1} of protein).

The GSSH: sulfite sulfurtransferase activity of DUF442 was measured for the production of thiosulfate, as reported [11]. Briefly, the reaction mixture contained 1 mM GSSH, 250 μM sulfite, and 50 μM DTPA in the Tris buffer. DTPA was added to chelate trace transition metals. dDUF442 was added at 0.05 mg per mL to initiate the reaction at 25 °C for 10 min. The membrane fractions containing SQR_{Cp} were also tested. The produced thiosulfate was derived with mBB (monobromobimane) and analyzed using HPLC. One unit (U) of RHOD activity was defined to form 1 nmol thiosulfate per 1 min.

2.7. SQR activity assay

The activity of SQR_{Cp} relies on the electron transport chain in cell membrane [40,41], and the prepared crude membrane fraction was sufficient to detect SQR activity [42]. In order to maintain the SQR_{Cp} activity as in native state, the membrane factions of SQR_{Cp} or SQR_{Cp}-C94S proteins overexpression cells were extracted to characterize the enzyme activity in all the biochemical assay in vitro.

The membrane fractions or whole cells containing SQR_{Cp} and SQR_{Cp}-C94S were prepared as described above. Then, they were used to oxidize sulfide in 50 mM Tris-HCl (pH 7.4) with 50 μM DTPA. The cells were normally at OD_{600} = 2 and the membrane fractions were used as indicated in the text. One mM sulfide was added into the mixtures to initiate the reaction, and the remained sulfide at different time points was determined by a colorimetric method [43]. One unit (U) of SQR activity was defined to consume 1 nmol sulfide per 1 min.

2.8. PDO activity assay

PDO activity was analyzed by using two methods. The first method was carried out by detecting oxygen consumption, and the other method was by determining the production of sulfite as in our previous report [11,16]. GSSH was prepared by mixing equal volumes of 17 mM glutathione in 50 mM potassium phosphate buffer at pH = 7.4 with a saturated sulfur solution in acetone, containing about 17 mM dissolved elemental sulfur [44]. The reaction was carried out in 50 mM Tris-HCl buffer (pH 7.4) containing 1 mM GSSH. 0.1 mg/mL PDO was added to initiate the reaction. Oxygen consumption was directly monitored using an Orion RDO meter (Thermo Scientific, USA). The RDO meter was calibrated with air-saturated water according to the manufacturer's instructions. One unit (U) of PDO activity was defined to consume 1 nmol oxygen per 1 min. The produced sulfite was derived with mBB (monobromobimane) and detected by HPLC according to a published method [11]. One unit (U) of PDO activity was also defined to generate 1 nmol sulfite per 1 min if indicated in the text.

2.9. Western blotting analysis of recombinant proteins

The western blotting procedure followed a reported method [45]. The proteins from the lysate were separated through a 12% SDS-PAGE gel and transferred onto a polyvinylidene fluoride (PVDF) membrane (Sangon, Shanghai, China) at 100 V and 4 °C for 60 min. The recombinant proteins with the His-tag were detected by using anti-His antibody conjugated with horseradish peroxidase (Sangon, Shanghai, China) and the high sensitive ECL luminescence reagent (Sangon, Shanghai, China); fluorescence intensity was detected and quantified by using a transilluminator (Fluor Chem Q; Protein Simple, San Jose, CA).

2.10. Sulfide spiking assay with whole cells and products analysis

The sulfide spiking assay was used to investigate the function of DUF442 inside cells during sulfide oxidation by SQR and PDO. It was done by using our previously established method [9]. Shortly, 15 mL whole cells were prepared and transferred to a 50-mL falcon tube. One mM sulfide was added to initiate the reaction. The mixture was incubated at 30 °C with gently shaking. The sulfide, cellular sulfane sulfur, sulfite, and thiosulfate were analyzed at various time intervals. The sulfide was determined by a colorimetric method [46], and cellular sulfane sulfur was analyzed by a previously used method [47]. Thiosulfate and sulfite were derived with mBB and detected by HPLC according to a reported method [9].

2.11. The determination of activity ratio of SQR_{Cp} to PDO_{Cp} in native C. pinatubonensis JMP134 or recombinant E. coli strains

The activity ratio is closely related with the enzyme expression levels of SQR_{Cp} and PDO_{Cp} inside cells. The use of cell lysates and crude membrane fractions would reflect the expression levels of both enzymes.

Fresh colonies of *C. pinatubonensis* JMP134 or recombinant *E. coli* strains were picked and incubated in LB medium overnight at 30 °C. The cultures were transferred into fresh LB medium with 1:100 dilution and cultured to OD_{600} = 0.8 at 30 °C. The *C. pinatubonensis* cells were induced with 50 μM NaHS every 20 min for 5 times, and the *E. coli* cells were induced with 0.4 mM IPTG for 4–5 h. The cell lysates and membrane fractions were prepared by using procedures as described above. The membrane fractions was used to determine SQR_{Cp} activity as described above. After membrane fraction was removed, the residual cell lysate was used to determine PDO_{Cp} activity by monitoring oxygen consumption as reported above. The protein concentrations in cell lysate and membrane fractions were determined by using the BCA method (Beyotime, China), and they were used to calculate the specific activities of SQR_{Cp} to PDO_{Cp}.

2.12. The measurement of glutathione (GSH), glutathione disulfide (GSSG), glutathione polysulfide (GS_nH, $n \geq 2$)

The detection of cellular GSH and GSSG detection was adopted from a previous report [48]. Briefly, the cell pellet harvested from 1 mL of cell suspension at OD_{600} = 10 was resuspended and shocked for 2 min in 200 μL of the stock buffer (143 mM sodium phosphate, 6.3 mM EDTA, pH 7.4) and 100 μL of 10% 5-sulfosalicylic acid. Cell debris and precipitated proteins were removed by centrifuging at 12,000×*g* for 3 min. Then, 5,5′-dithiobis(2-nitrobenzoic acid) (DTNB)-GSSG reductase recycling method [49] was adopted to measure GSH and GSSG levels by using a commercial kit (Beyotime, China).

GS_nH was treated with 50 mM HPE-IAM (β-(4-hydroxyphenyl)ethyl iodoacetamide) in 10 mM phosphate buffer (pH 7.4) at 37 °C for 1 h in

dark. The alkylated adducts were detected by using LC-ESI-MS/MS by the LCMS-8050 Nexera UHPLC system (Shimadzu) with a C18 column (VP-ODS, 150 × 4 mm, Shimadzu) with a reported elution procedure (*11*). The adducts of GSH (GS-adduct), GSH persulfide (GSS-adduct), GSH trisulfide (GSSS-adduct), GSH tetrasulfide (GSSSS-adduct), and pentasulfide (GSSSSS-adduct) were detected and compared by relative intensity.

2.13. Molecular docking of GS_nH into the catalytic pocket of PpPDO

Autodock Vina was used according to the instructions. Briefly, the structure of PDO_{Pp} complexed with GSH (PDB ID = 4YSL) was used as a receptor after the ligand GSH was removed, and GS_nH (n = 2–5) was then used as the ligand. The PDBQT files of the receptor and ligand were generated by adding polar hydrogen and partial charges to them. The grid parameters were delineated (center_x = −26.75 Å, center_y = 26.66 Å, center_z = −17.42 Å, size_x = 24.5 Å size_y = 24.5 Å, size_z = 24.5 Å). H74, D78, H149, D170, F173, Y177, T149, R181, F184, H212, Y214, H236, R250, R253, L257, M259, V261, and L262 in the receptor were selected as flexible residues. The molecular docking was run with these parameters for several rounds by changing the random seeds until a reasonable docking position of GS_nH appeared.

2.14. Bioinformatics

The genes encoding the RHOD domains were searched in the *sqr-pdo* operons among the 441 strains in our previous report [9]. First, all the corresponding SQR and PDO sequences were collected. Then, proteins with an RHOD domain were identified by using the conserved domain function from NCBI website. 460 proteins had a potential RHOD domain. The RHOD domains that did not have the conserved cysteine at the active site or did not have complete sequences were excluded. 126 representative proteins included 37 PDO-RHOD fusion proteins, 50 SQR-RHOD fusion proteins, and 39 dissociated RHODs were collected by using CD-Hit of 90% similarity as the threshold. These annotated RHOD domains were aligned using ClustalW 2.1 with known RHOD domain sequences in GlpE, PspE, YgaP from *Escherichia coli*, CstB from *Staphylococcus aureus*, PRF from *Burkholderia phytofirmans*, RDL1, RDL2 from *Saccharomyces cerevisiae* and TSTD1, TSTD2, TSTD3 from human were used as standards. A phylogenetic tree was constructed by a neighbor-joining method using MEGA 7.0, with a partial deletion, p-distance distribution, and bootstrap at 1000 repeats.

16 and 72 protein sequences of known PDO were collected from our previously published two papers with known outgroups [9,11]. Five protein sequences with published structures were also collected and used for phylogeny analysis with similar parameters as that used for RHOD (*vide supra*). Representative PDO sequences from distant clades in the phylogenetic tree were collected and used for multiple sequence alignment by using Clustal Omega [50].

2.15. Statistical analysis

Statistical analysis was done using GraphPad Prism 9.0. Data in more than two groups were analyzed using independent one-way analysis of variance (ANOVA) to calculate the adjusted p values; the p-value $<$ 0.033 indicated statistical significance. The significant difference between the two groups was analyzed using an independent student's t-test; the p-value $<$ 0.05 indicated statistical significance.

3. Results

3.1. Optimizing the expression ratio of SQR_{Cp} and PDO_{Cp} in RHOD-free E.coli to imitate their expression levels in C. pinatubonensis JMP134

Nine native genes coding for RHODs or proteins with RHOD domains were sequentially deleted in *E. coli* MG1655 (Fig. S1). The strain with all 9 genes deleted (9K) grew slowly, but the strain with 8 RHOD genes except *thiI* being deleted (8K) grew equally well as the wild type (Fig. S3A). ThiI is involved in the biosynthesis of both thiamin and 4-thiouridine that is present in tRNA [22]. The RHOD activity in cell extracts of *E. coli* 8K was significantly decreased in comparison with the wild type strain (Fig. S3B). When the nine genes were individually overexpressed in *E. coli* 8K, the cell extracts containing overexpressed GlpE, PspE, or YgaP showed increased RHOD activity (Fig. S3B), but the others did not (Data not shown). *E. coli* 8K was selected as the host to investigate the physiological function of the RHOD or RHOD domain during sulfide oxidation.

To investigate the function of the DUF442 domain (fDUF442) in SQR_{Cp}, the activity ratio of SQR and PDO in recombinant *E. coli* should be similar to that in *C. pinatubonensis* JMP134. In our first design, the *pdo* and *sqr* genes from *C. pinatubonensis* JMP134 were cloned into vector pBBR1MCS-2 as P_{lac}-n*pdo*$_{Cp}$-n*sqr*$_{Cp}$, in which the two genes were under the control of lac promoter (Plac) and the native ribosome binding sites (RBSs) (Fig. S2). When tested, the ratio of the specific activities of SQR and PDO in cell extracts of *E. coli* 8K was 3.7 fold higher than that in its native strain *C. pinatubonensis* JMP134 (Table 1). Three artificial RBS sequences with defined strength were applied to reduce the expression level of SQR_{Cp} (Fig. S2). When RBS a3 was used, the SQR_{Cp} activity was decreased and the ratio of SQR and PDO activities in cell extracts was 1.0, similar to that in *C. pinatubonensis* JMP134 (Table 1). Hence, this new expression cassette Plac-n*pdo*$_{Cp}$-a3*sqr*$_{Cp}$ in *E. coli* 8K (*E. coli* 8K-nPDO$_{Cp}$-a3SQR$_{Cp}$) was used to characterize the function of fDUF442.

3.2. The DUF442 domain of SQR_{Cp} minimized the accumulation of sulfane sulfur during sulfide oxidation by SQR_{Cp} and PDO_{Cp} in E. coli

The DUF442 domain of SQR_{Cp} (fDUF442) is a functional rhodanese when produced as a dissociated protein (dDUF442) [11]. The rhodanese function of fDUF442 in SQR_{Cp} was inactivated by mutating Cys^{94} to Ser (C94S). Sulfide oxidation by *E. coli* 8K-nPDO$_{Cp}$-a3SQR$_{Cp}$ and *E. coli* 8K-nPDO$_{Cp}$-a3SQR$_{Cp}$-C94S cells was tested. *E. coli* 8K-nPDO$_{Cp}$-a3SQR$_{Cp}$-C94S cells had an increased rate of sulfide oxidation with increased levels of sulfane sulfur and thiosulfate but reduced sulfite production in comparison with *E. coli* 8K-nPDO$_{Cp}$-a3SQR$_{Cp}$ (Fig. 1A–D). By contrast, the mutation (C94S) effect was not apparent when the wild-type *E. coli* MG1655 was used as the host (Fig. S4), suggesting RHOD activity in *E. coli* MG1655 compensates the DUF442 activity loss in SQR$_{Cp}$-C94S (Fig. 1A&B). The dDUF442 protein from another vector partially compensated the C94S mutation in *E. coli* 8K-nPDO$_{Cp}$-a3SQR$_{Cp}$-C94S/dDUF442 during sulfide oxidation with reduced sulfane sulfur accumulation and decreased thiosulfate production as well as increased sulfite production (Fig. 1A–D). Further, *E. coli* rhodaneses GlpE and YgaP on the second plasmid partially complemented the C94S mutation in *E. coli* 8K-nPDO$_{Cp}$-a3SQR$_{Cp}$-C94S, but PspE did not (Fig. S5). PspE is a periplasmic rhodanese [51], and its location is likely the cause for the lack of complementation, as the active site of SQR_{Cp} is on the cytoplasmic side of the membrane [42]. dDUF442 had strong RHOD activity and catalyzed the reaction between GSSH and sulfite to produce

Table 1
The specific activities of SQR_{Cp} and PDO_{Cp} of three strains.[a].

	E. coli 8K-nPDO$_{Cp}$-nSQR$_{Cp}$	*E. coli* 8K-nPDO$_{Cp}$-a3SQR$_{Cp}$	*C. pinatubonensis* JMP134
SQR_{Cp}	93.3 ± 2.4	45.3 ± 4.8	9.3 ± 1.2
PDO_{Cp}	44.4 ± 3.3	45.3 ± 3.6	15.0 ± 0.1
SQR_{Cp}/ PDO_{Cp}	2.2	1.0	0.6

[a] *E. coli* strains were cultured in LB and induced by IPTG; *C. pinatubonesis* JMP134 was cultured in LB and induced by H_2S. Cells were harvested and lysed. After ultracentrifugation, SQR was in the pellet with the membrane fraction, and PDO was in the supernatant. Their activities (μmol/min/mg of protein) were determined.

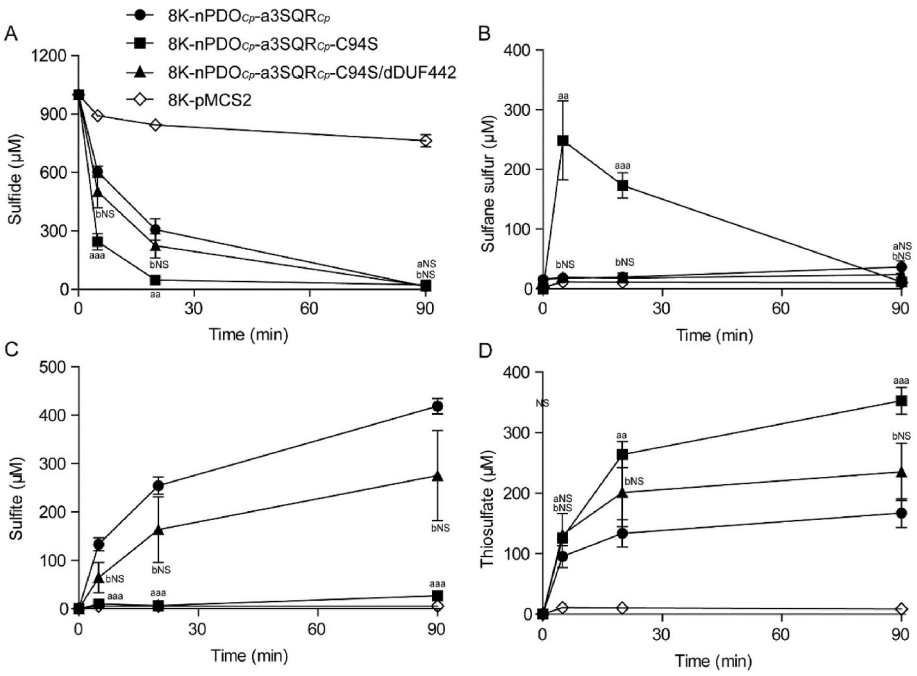

Fig. 1. The function of DUF442 during sulfide oxidation by SQR$_{Cp}$-PDO$_{Cp}$ in *E. coli* 8K. The induced recombinant cells were prepared as resting cells in Tris buffer at OD_{600} of 2. 1 mM sulfide was added to initiate the reaction. The residual sulfide and products were analyzed at defined time intervals. **A**) Sulfide; **B**) Sulfane sulfur; **C**) Sulfite; **D**) Thiosulfate. Data are averages and standard deviations of three parallel experiments. The one-way ANOVA method was used to calculate the *p*-value ('aa' = $p < 0.002$, 'aaa' = $p < 0.001$, and 'aNS/bNS' = no significance) of an indicated pair of groups adjusted by the Dunnett method as statistical hypothesis testing. If the character 'a' was contained to represent an adjusted *p*-value, a significant difference was observed between 8K-nPDO$_{Cp}$-a3SQR$_{Cp}$-C94S and 8K-nPDO$_{Cp}$-a3SQR$_{Cp}$. If character 'b' was contained to represent an adjusted *p*-value, it represented the significant difference between 8K-nPDO$_{Cp}$-a3SQR$_{Cp}$-C94S/dDUF442 and 8K-nPDO$_{Cp}$-a3SQR$_{Cp}$.

thiosulfate (Fig. S6), but the membrane fraction containing SQR$_{Cp}$ had very low rhodanese activity and did not catalyze the reaction of GSSH with sulfite to produce thiosulfate, suggests that dDUF442 and fDUF442 act differently during sulfide oxidation by SQR$_{Cp}$ and PDO$_{Cp}$.

When cellular GSH and GSSG during sulfide oxidation were analyzed, GSH levels were gradually decreased in *E. coli* 8K-nPDO$_{Cp}$-a3SQR$_{Cp}$, but rapidly reduced in *E. coli* 8K-nPDO$_{Cp}$-a3SQR$_{Cp}$-C94S during the initial phase of sulfide oxidation (Fig. 2). When dDUF442 was supplied via another plasmid, the rapid oxidation of GSH was partially alleviated (Fig. 2). The rapid oxidation of GSH to GSSG causes disulfide stress to cells (*52*).

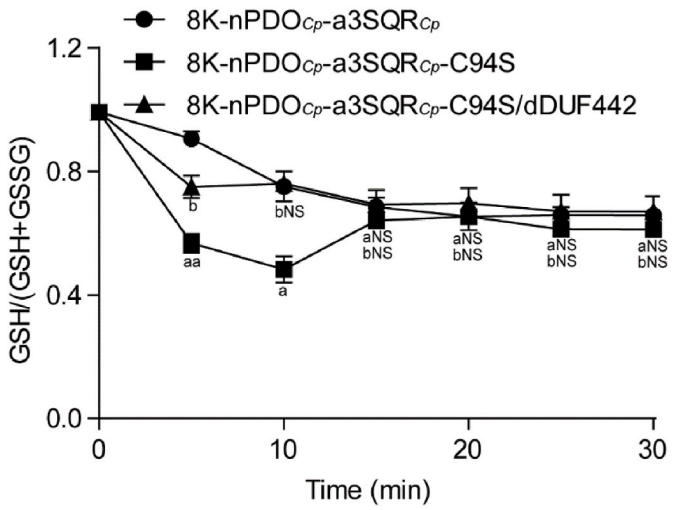

Fig. 2. The transitory reduction of cellular GSH during sulfide oxidation. The induced recombinant *E. coli* cells were resuspended in Tris buffer with 50 μM DTPA to obtain resting cells. Sulfide was added at 1 mM to initiate the reaction. The cellular reduced GSH and total GSH content (GSH + GSSG) were measured. Data are averages and standard deviations of three parallel experiments. The one-way ANOVA method was used to calculate the *p*-value ('a'/'b' = $p < 0.033$, 'aa' = $p < 0.002$, and 'aNS/bNS' = no significance) of two groups of data adjusted by the Dunnett method. If the character 'a' was contained to represent an adjusted *p*-value, it was used to show the significant difference between 8K-nPDO$_{Cp}$-a3SQR$_{Cp}$-C94S and 8K-nPDO$_{Cp}$-a3SQR$_{Cp}$. If character 'b' was contained to represent adjusted *p*-value, it represented the significance difference between 8K-nPDO$_{Cp}$-a3SQR$_{Cp}$-C94S/dDUF442 and 8K-nPDO$_{Cp}$-a3SQR$_{Cp}$.

3.3. *fDUF442 modulated SQR$_{Cp}$ activity to prevent cellular sulfane sulfur accumulation*

E. coli 8K carrying pBBR1MCS-2 with P_{lac}-n*sqr*$_{Cp}$ (*E. coli* 8K-nSQR$_{Cp}$) and *E. coli* 8K-nSQR$_{Cp}$-C94S were induced to express SQR$_{Cp}$ and SQR$_{Cp}$-C94S, respectively. The expression levels of SQR$_{Cp}$ and SQR$_{Cp}$-C94S in the cells were similar according to the western blotting analysis (Fig. S7). At the same cell density, *E. coli* 8K-nSQR$_{Cp}$-C94S had a higher sulfide oxidation activity than *E. coli* 8K-nSQR$_{Cp}$, and the complementation of dDUF442 via another plasmid did not slow down sulfide oxidation by *E. coli* 8K-nSQR$_{Cp}$-C94S/dDUF442 (Fig. 3A). The membrane fractions containing SQR$_{Cp}$-C94S also oxidized sulfide faster than with SQR$_{Cp}$ did, but the difference was small (Fig. 3B). The kinetic parameters of SQR$_{Cp}$ and SQR$_{Cp}$-C94S were determined by using the corresponding membrane fractions (Table S3). GSH greatly increased sulfide oxidation by SQR$_{Cp}$-C94S, but not by SQR$_{Cp}$ (Fig. 3B). Sulfite stimulated sulfide oxidation by the membrane fractions containing SQR$_{Cp}$ and SQR$_{Cp}$-C94S, but the effect was smaller than GSH (Fig. S8A). dDUF442 did not affect sulfide oxidation by SQR$_{Cp}$-C94S with or without GSH or sulfite (Fig. S8B).

The structure of SQR$_{Cp}$ was built via homologous modeling by using AlphaFold2 (Fig. 4), and the active site (Cys310 and Cys490) of the SQR domain and the active site Cys94 of the DUF442 domain were facing each other with a distance between the Cys94 thiol to the Cys310 and Cys490 thiols at 33.7 Å and 30.4 Å, respectively. The distance between the Cys310 and Cys490 thiols was 3.3 Å. The linker of the SQR and DUF442 domains predicted by AlphaFold2 had a low prediction score, suggesting a flexible region (Fig. 4A). fDUF442 could swing around the SQR domain and move into the above position of the active pocket. Hence, Cys94 might receive sulfane sulfur from the active site (Cys310 and Cys490) and then pass it to GSH. The rate of sulfur transfer was modulated by fDUF442. When Cys94 was mutated to Ser94, the mutated fDUF442 was no longer attracted by the active site (Cys310 and Cys490). A slight move of fDUF442 could create room for GSH to have

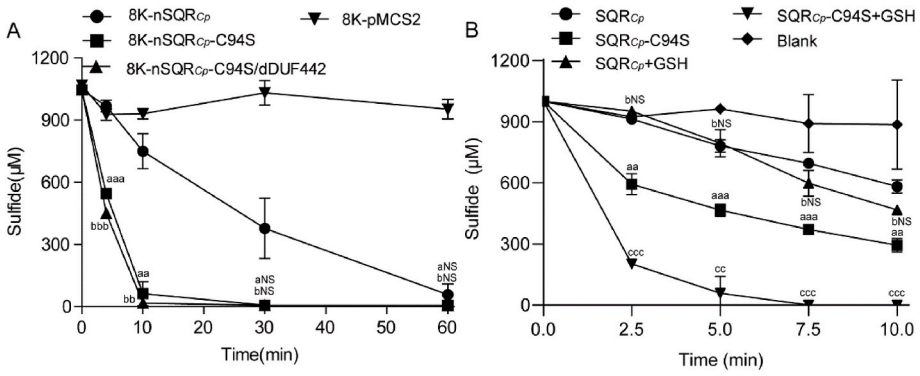

Fig. 3. The effects of fDUF442 and dDUF442 on sulfide oxidation by SQR_{Cp} and SQR_{Cp}-C94S, respectively. The induced *E. coli* 8K-nSQR$_{Cp}$ and *E. coli* 8K-nSQR$_{Cp}$-C94S cells were used to obtain resting cells and membrane fractions. **A**) Sulfide oxidation by whole cells at OD_{600} of 2. **B**) Sulfide oxidation by membrane fractions at 0.3 mg of protein per mL in Tris buffer with or without 1 mM GSH. Adding dDUF442 did not affect sulfide oxidation with or without GSH (Fig. S8). The Tris-HCl buffer was used as the blank. Data are averages and standard deviations of three parallel experiments. The one-way ANOVA method was used to calculate the *p*-value ('aa'/'bb'/'cc' = $p < 0.002$, 'aaa'/'bbb'/'ccc' = $p < 0.001$, and 'aNS/bNS/cNS' = no significance) of two groups of data adjusted by the Dunnett method (A) and Sidak method (B) as statistical hypothesis testing. For A), character 'a' was used to show the significant difference between 8K-nPDO$_{Cp}$-a3SQR$_{Cp}$-C94S and 8K-nPDO$_{Cp}$-a3SQR$_{Cp}$, and character 'b' represents the difference between 8K-nPDO$_{Cp}$-a3SQR$_{Cp}$-C94S/dDUF442 and 8K-nPDO$_{Cp}$-a3SQR$_{Cp}$. For B), character 'a' was used to show the significant difference between SQR$_{Cp}$-C94S and SQR$_{Cp}$, and character 'b' represented the difference between SQR$_{Cp}$ + GSH and SQR$_{Cp}$, and character 'c' represented the difference between SQR$_{Cp}$-C94S + GSH and SQR$_{Cp}$-C94S.

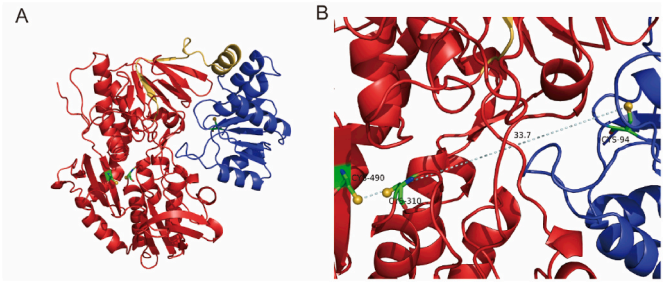

Fig. 4. Crystal structure of SQR_{Cp} simulated by AlphaFold2. A) The structure of an SQR$_{Cp}$ monomer consists of the C-terminal SQR domain (red), a linker region (yellow), and the N-terminal DUF442 domain (blue). **B**) The distance of the active sites of the two domains. (For interpretation of the references to color in this figure legend, the reader is referred to the Web version of this article.)

access to the active site, which should facilitate the removal of the sulfane sulfur from the active site and increase the enzymatic turnovers.

3.4. *dDUF442 enhanced PDO$_{Cp}$ activity to avoid sulfane sulfur accumulation*

The effect of dDUF442 on PDO$_{Cp}$ activity was tested. Total sulfite content (TSC), the sum of thiosulfate and sulfite, was used to calculate PDO activity because sulfite spontaneously reacts with sulfane sulfur to produce thiosulfate [11]. PDO$_{Cp}$ and dDUF442 oxidized GSSH to TSC much more quickly than PDO$_{Cp}$ did (Fig. 5A). With dDUF442 at M ratios (dDUF442: PDO$_{Cp}$) of 0.1:1 and 1:1, the specific PDO activity increased 1.7 and 4.5 folds. At a molar ratio of PDO$_{Cp}$ and dDUF442 of 1:1, dDUF442 significantly increased the V_{max} value of PDO$_{Cp}$ and slightly increased its Km value for GSSH with overlapping error bars (Table 2). Sulfite was gradually accumulated to 40 μM and 20 μM during GSSH oxidation by PDO$_{Cp}$ and PDO$_{Cp}$ with dDUF442 (Fig. 5A). The effect of sulfite on PDO$_{Cp}$ was further tested, and the addition of 1 and 10 mM sulfite did not affect PDO$_{Cp}$ activity (Fig. S9), suggesting that sulfite should not affect PDO$_{Cp}$ activity with or without dDUF442. We then tested sulfide oxidation by SQR$_{Cp}$-C94S and PDO$_{Cp}$ with or without dDUF442. As expected, sulfane sulfur was not accumulated and more TSC was produced when dDUF442 was present (Fig. 5B).

When the sulfane sulfur produced by SQR$_{Cp}$-C94S in the presence of GSH was tested, and longer chain GS_nH, GS_nG, and H_2S_n were detected with dDUF442 than without dDUF442 (Fig. 6 &Table S4). Further, dDUF442 decreased GSSG production (Fig. 6F). Thus, we suspected that PDO might prefer to use long-chain GS_nH to short-chain GS_nH, as

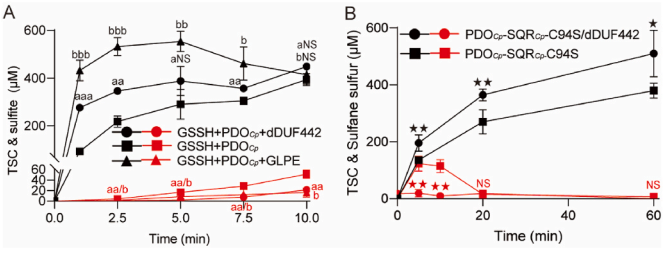

Fig. 5. dDUF442 promoted PDO activity. A) To initiate the reaction, GSSH was added at 1 mM to Tris buffer with PDO$_{Cp}$, PDO$_{Cp}$, and dDUF442 or GlpE. **B**) Sulfide oxidation by the membrane containing SQR$_{Cp}$-C94S and PDO$_{Cp}$ with or without dDUF442 in Tris buffer with 1 mM GSH. The SQR$_{Cp}$-C94S membrane and PDO$_{Cp}$ were added at 0.3 and 0.1 mg of protein per mL to simulate their activity ratio *in vivo*, and dDUF442 was used at molar ratios (dDUF442: PDO$_{Cp}$) of 1:1. TSC (sulfite and thiosulfate) (black) and sulfite or sulfane sulfur (red) were determined at different time intervals. Data are averages and standard deviations of three parallel experiments. The one-way ANOVA method was used to calculate the *p*-value ('b' = $p < 0.033$, 'aa'/'bb' = $p < 0.002$, 'aaa'/'bbb' = $p < 0.001$ and 'aNS/bNS' = no significance) of two groups of data adjusted by the Dunnett method (A) and Sidak method (B) as statistical hypothesis testing. For A), character 'a' was used to show the significant between PDO$_{Cp}$ + GSSH + dDUF442 and PDO$_{Cp}$ + GSSH, and character 'b' represented the significant difference between PDO$_{Cp}$ + GSSH + GlpE and PDO$_{Cp}$ + GSSH. Black symbols represented the difference of TSC values, and red symbols represented the difference between sulfite (A) or sulfane sulfur (B). (For interpretation of the references to color in this figure legend, the reader is referred to the Web version of this article.)

Table 2
Kinetic parameters of PDO$_{Cp}$ with or without dDUF442.

	Vmax μM/(min·mg)	Km μM GSSH	Kcat S^{-1}	Kcat/Km $mM^{-1}\cdot S^{-1}$
PDO$_{Cp}$	67.6 ± 20.1	288.9 ± 98.5	37.1	128.4
PDO$_{Cp}$ + dDUF442	375.3 ± 103.6	384.9 ± 122.2	205.7	534.4
p	***	NS	**	***

The assays were done with changing GSSH concentrations in 50 mM Tris-HCl (pH = 7.4) buffer containing 50 μM DTPA. GSSH was freshly prepared under anoxic conditions. Data are averages of three parallel experiments with standard deviations. Unpaired Student's t-tests were performed to determine the difference between the two samples (** = $p < 0.05$, *** = $p < 0.01$, and NS = no significance).

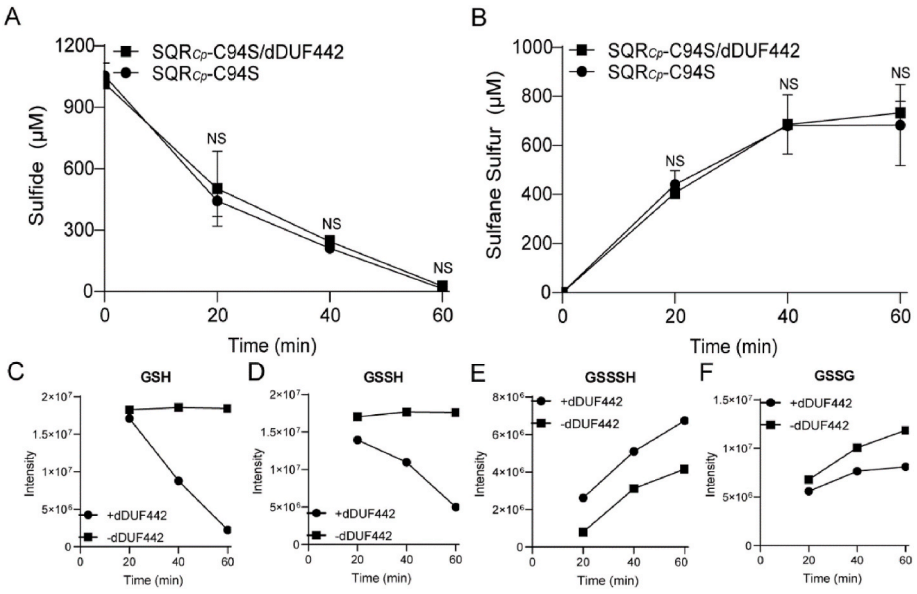

Fig. 6. dDUF442 promoted long-chain GS_nH formation during sulfide oxidation by SQR_{Cp}-C94S. The species of GS_nH produced from 1 mM sulfide oxidated by SQRCp-C94S at 0.15 mg of membrane protein per mL in the presence of 1 mM GSH with or without 0.05 mg per mL were alkylated by HPE-IAM and determined by LC-MS/MS. **A**) Sulfide; **B**) Sulfane sulfur; **C-E**) GS_nH (n = 1–3); **F**) GSSG. Dates were detected at defined time intervals. Data in **A)** and **B)** are averages and standard deviations of three parallel experiments. Unpaired Student's t-tests were performed to determine the difference between the two groups (NS = no significance).

dDUF442 stimulated the activity of PDO and the formation of longer chanin GS_nH.

3.5. The pocket in PDO could accept long-chain GS_nH as the substrate

We speculated that long-chain GS_nH may be a better substrate for PDO_{Cp}. Since the structure of PDO_{Cp} had not been determined, we simulated the structure of PDO_{Cp} from that of *Pseudomonas putida* PDO_{Pp} [53] by using the Swiss model. The sequence similarity between these two proteins is 81.9%. The structures of PDO_{Cp} and PDO_{Pp} were essentially the same (Fig. S10A). PDO_{Pp} has a deep catalytic pocket (Fig. S10B), which may relieve the steric hindrance of binding long-chain GS_nH. The structure of PDO_{Pp} complexed with GSH was then used to dock GS_nH. Interestingly, GS_nH (n = 2–5) was successfully docked into the catalytic pocket of PpPDO, and the spatial conformation of the GS_nH carbon skeleton is quite similar to that of GSH (Fig. 7), and the affinity was shown in Table S5. This result showed that GS_nH (n > 2) is also possible to enter this deep pocket to become a potential substrate of PDO_{Pp}.

PDOs are divided into three types [16]; both PDO_{Cp} and PDO_{Pp} belong to type II. The result of multiple sequence alignment showed that the amino acid residues composing the catalytic pocket of PDO_{Pp} are relatively conserved in both Type I and Type II of PDOs (Fig. S11), but not in type III PDOs that do not use GSSH as a substrate. Five protein structures of type I and type II PDOs are available, and they were diversely distributed in the PDO phylogenetic tree (Fig. S12). The type I PDO from human mitochondria (PDO_{Hm}) and PDO_{Pp} are distantly related with a sequence similarity lower than 40%. However, their tertiary structures were similar (Fig. S13A). The position of the Fe^{2+} atom in the pocket of PDO_{Hm} is even deeper than that in PDO_{Pp} (Figs. S13A and B). The conformation of the key residues composing the catalytic pockets and the vacuum electrostatics in the pockets are also similar (Figs. S13B–D). The results suggest that type I and II PDOs could use long-chain GS_nH as the substrate.

3.6. The types and distribution of RHOD domains in the SQR-PDO pathway

Previously, we have reported 454 *sqr-pdo* operons in 441 genomes from 4929 sequenced bacterial genomes (*9*). Here, we further analyzed genes encoding RHOD domains associated with the operons. Of the 454 operons and linked genes within 3 loci, 385 gene clusters contained 458

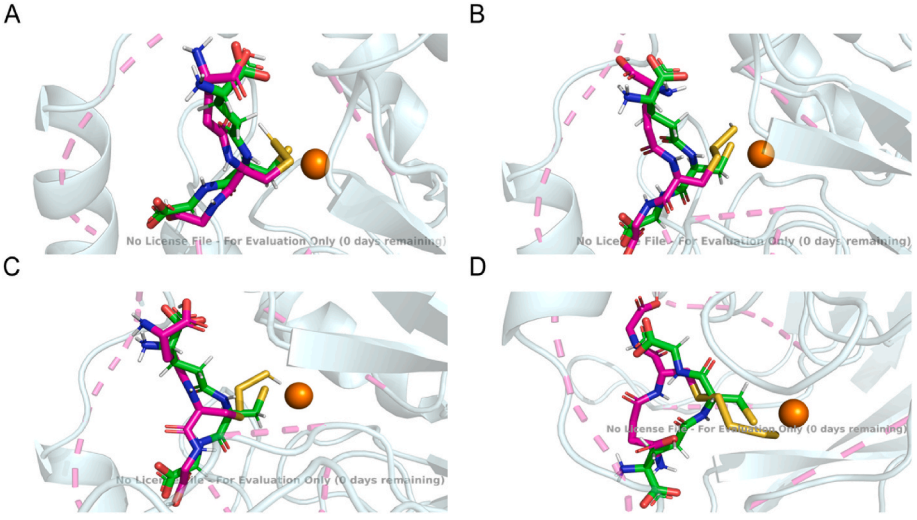

Fig. 7. The docking of GS_nH into the catalytic pocket of PDO_{Pp}. The flexible docking of GS_2H (A), GS_3H (B), GS_4H (C), GS_5H (D) into the catalytic pocket of PDO_{Pp}, aligned with the original pocket of PDO_{Pp} complexed with GSH. The carbon skeleton of the reported GSH was colored in green, and those of GS_nH (n ≤ 5) were colored in red. The flexible residues in PDO_{Pp} were shown in a dash-lined cartoon mode. (For interpretation of the references to color in this figure legend, the reader is referred to the Web version of this article.)

genes coding for 460 RHOD domains (Table S6). 204 SQRs and 166 PDOs were individually fused with one RHOD domain. The remaining 90 RHOD domains were encoded by 88 genes, as dissociated RHODs. (Table S7).

126 representative sequences of these RHOD domains were selected for phylogenetic tree analysis with known RHODs as references (Fig. S14). RHOD domains in SQRs were conserved in the same clade, and the associated SQRs were all distributed in Proteobacteria within five genera: *Acinetobacter*, *Burkholderia*, *Gluconobacter*, *Pseudomonas*, *Cupriavidus* (Table S7). Their active sites are highly similar (Fig. 8A); their associated gene clusters were also organized in the same way (Fig. S15). The Rhodanese domains that were either fused with PDO or as dissociated proteins did not form a clear clade (Fig. S14). The three *E. coli* rhodaneses GlpE, YgaP, and PspE were distributed in the different clades (Fig. S14). The sequences of the active sites of the RHOD domains fused with PDO and dissociated RHODs were relatively conserved (Fig. 8B&C). The PDOs fused with RHOD all belong to type III PDO (Table S7) [9].

4. Discussion

With a rhodanese-free *E. coli* strain, our results show that rhodanese prevents the accumulation of cellular sulfane sulfur during sulfide oxidation by SQR and PDO, explaining why rhodaneses or rhodanese domains are often associated with *sqr* and *pdo* genes. When a rhodanese domain is fused with SQR, such as SQR_{Cp}, it modulates SQR activity to prevent rapid production of cellular sulfane sulfur (Figs. 1 and 9A). The dissociated rhodaneses work differently by stimulating PDO activity to prevent the accumulation of cellular sulfane sulfur (Figs. 5 and 9B). The presence of rhodanese genes in *sqr* and *pdo* gene clusters is an indication of the necessity of keeping cellular sulfane sulfur low.

Our results indicate that RHOD is not necessary for thiosulfate production (Fig. 1). The results may seem to contradict previous reports. In vitro tests have shown that dDUF442 and the human mitochondrial rhodanese catalyze the reaction between sulfite and GSSH to producce thiosulfate [13,54], and the RHOD domain of CstB converts CoA-SSH and sulfite to thiosulfate [15]. We believe that RHOD may play several roles during sulfide oxidation by SQR and PDO. Without RHOD, sulfane sulfur, including GSnH and HSnH, is accumulated (Fig. 1). The produced sulfite spontaneously reacts with HSnH to produce thiosulfate, and this reaction is not catalyzed by RHOD (*11*). Further, sulfite may function as an acceptor to directly receive a sulfane sulfur from SQR (Fig. S8A) [41]. As a result, sulfite is not accumulated (Fig. 1C), and thiosulfate producton is increased (Fig. 1B). In the presence of RHOD, it stabilizes long chain GSnH (Fig. 6C–F), converts HSnH to GSnH [11], and catalyzes the formation of thiosulfate between GSnH and sulfite [11, 13,15]. From a physiological perspective, the lack of RHOD activities leads to the accumulation of sulfane sulfur, which is detrimental to the cells (Fig. 9).

Excessive cellular sulfane sulfur is toxic, causing rapid GSH oxidation (Fig. 2). GSSH reacts with GSH to produce GSSG and H_2S, and glutathione reductase reduces GSSG back to GSH at the expense of NADPH [55]. This GSH and glutathione reductase mediates sulfur reduction is proposed as a detoxification mechanism for fungi to resist elemental sulfur, a common fungicide. When glutathione reductase is inactivated in fungi, the mutants are more sensitive to elemental sulfur [55]. OxyR is known to respond to H_2O_2 stress [48], and exposure to polysulfide also activates OxyR that upregulates the expression of genes coding for the removal of cellular sulfane sulfur in *E. coli* [56].

Thus, accumulating GSSG or other disulfides is harmful to microorganisms, and it causes disulfide stress [52]. Disulfide formation inside cells is often triggered by exposure to the synthetic diamide [diazenedicarboxylic acid bis(N, N-dimethylamide)] [57,58]. HOCl that is produced by neutrophils is another agent to induce disulfide formation [59,60]. H_2O_2 is also an inducer for disulfide formation, but the rate is slow [61]. Further, cystine uptake is likely a common situation that can quickly evoke disulfide stress [62]. Here, we found that the accumulation of cellular sulfane sulfur is new stress that triggers disulfide formation. The disulfide stress leads to the formation of proteins with disulfide bonds that may inactivate their functions [62]. OxyR senses increased levels of cellular sulfane sulfur and turns on the expression of genes encoding enzymes, such as thioredoxin, glutaredoxin, and catalase, for the removal of sulfane sulfur [56]. OxyR also senses disulfide formation induced by cystine uptake [62]. Thus, sulfane sulfur is an inducer of disulfide stress and bacteria like *E. coli* have defense mechanisms to cope with it.

The function of fDUF442 is to modulate SQR_{Cp} activity (Fig. 3A). Our

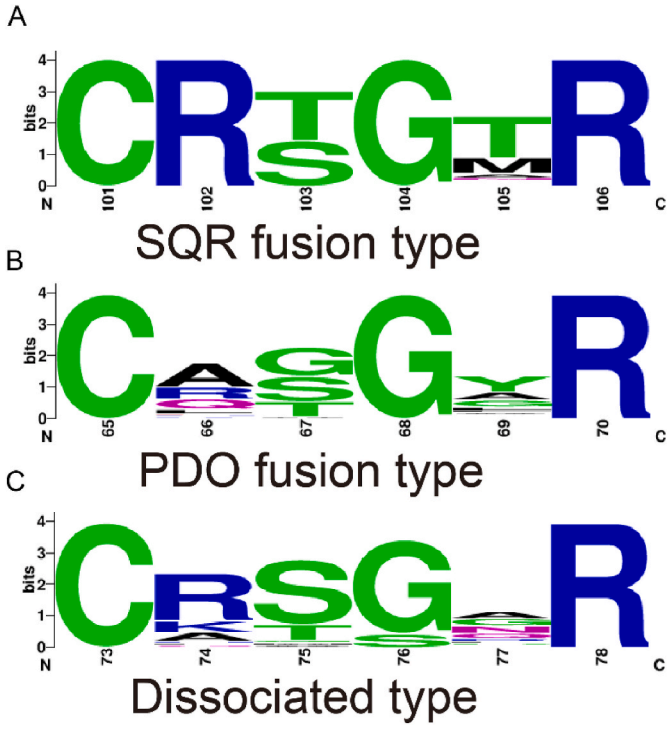

Fig. 8. Sequence logo of the active site in the three types of RHOD domains.

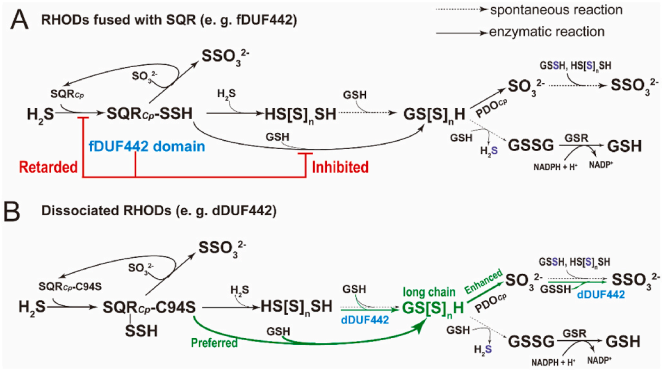

Fig. 9. The schematic diagram for the functions of DUF442 in SQR_{Cp}-PDO_{Cp} pathway. A) The fDUF442 domain retarded the sulfide oxidation activity of SQR_{Cp} by avoiding giving sulfane sulfur to GSH. The accumulation of GSSH was avoided to reduce invalid GSH oxidation. **B**) The SQR_{Cp}-C94S preferred to use GSH as an acceptor. The dDUF442 could increase the formation of long-chain thioalkylated GSH, which is preferred by PDO as a substrate to enhance the oxidation rate of sulfane sulfur. The red line with the stop character indicated the repression effect by fDUF442. The green line with the arrow indicated the acceleration effect by dDUF442. (For interpretation of the references to color in this figure legend, the reader is referred to the Web version of this article.)

mutational analysis showed that the inactivation of the active site of the fDUF442 domain enhanced the SQR activity and allowed direct access of GSH to the active site of the SQR domain (Fig. 3B). The results suggest that fDUF442 modulates the release of sulfane sulfur from the active site of the SQR domain to avoid the production of excessive GSSH that spontaneously reacts with GSH to generate H_2S and GSSG. Considering sulfane sulfur was mainly produced in cells, the cellular concentration of GSH would become much lower along with sulfide oxidation. Although the nonenzymatic reduction of cellular sulfane sulfur back to H_2S by GSH is fast, the cellular GSH content is quite limited in comparison with the concentrated sulfane sulfur in cells. Hence, without PDO, *E. coli* (SQR_{Cp}) oxidized H_2S finally to cellular sulfane sulfur, including polysulfide and GS_nH (Fig. 6 & Table S4) [11]. In the presence of PDO, the regulated production of GS_nH is consumed by PDO to avoid the accumulation of cellular sulfane sulfur (Fig. 1).

The dDUF442 also prevents the accumulation of cellular sulfane sulfur via a different mechanism (Fig. 9B). It speeds up PDO_{Cp} activity by several folds so that excessive cellular sulfane sulfur is not accumulated (Fig. 5 & Table 2). Given the binding pockets of type I and type II PDOs, including PDO_{Cp} and PDO_{Pp}, are similar and can accommodate GSH as well as long-chain GS_nH (Fig. 7), we speculate these PDOs bind GS_nH and successively oxidize the terminal sulfur to sulfite until GSH is produced. Since the affinities of GSH and GS_nH to PDO_{Pp} are similar (Table S5), the release of GSH may be a limiting step. When GSH is released, another GS_nH enters the active site of PDO_{Pp} to start another round of oxidation. Thus, each cycle of substrate binding will lead to more sulfur oxidation for a long-chain GS_nH than GSSH. This hypothesis is consistent with our results that dDUF442 mainly affects the K_{cat} of PDO_{Cp}, but not its K_m for GS_nH (Table 2). Thus, type I and II PDOs may prefer to use long-chain GS_nH as the substrate.

The mechanism of SQR has been elucidated with the human mitochondrial SQR (SQR_{Hm}) [63]. The active site of SQR_{Hm} consists of two cysteine residues that form a trisulfide linkage; the addition of H_2S produces 2 persulfides (2xCys-SSH); one Cys-SSH reduces FAD, and the other passes the sulfane sulfur to a sulfane sulfur acceptor. Various compounds, such as sulfide, GSH, and sulfite, can receive the sulfane sulfur to produce HSSH, GSSH, and thiosulfate, respectively [13,41,54,64]. Since GSH enhances SQR_{Hm} activity, GSH is likely the preferred sulfane sulfur receptor for the enzyme (*13, 23*). Since GSH does not speed up SQR_{Cp} activity (Fig. 3B), GSH may not be a preferred sulfane sulfur acceptor. SQR_{Cp} may pass the sulfane sulfur to H_2S or sulfite (Fig. S8). We speculate that fDUF442 may prevent GSH from accessing the Cys-SSH at the active site of SQR_{Cp} (Fig. 9), but it does not affect the access of sulfite (Fig. S8). When the active Cys residue of fDUF442 is mutated to Ser, the mutant protein SQRCp-C94S favors GSH as the sulfane acceptor (Fig. 3B). Further, SQRCp-C94S has increased Vmax and decreased Km over SQR_{Cp}, which leads to a significantly increased catalytic efficiency for SQR_{Cp}-C94S (Table S3). The results suggest that fDUF442 modulates the release of sulfane sulfur and slows down sulfide oxidation. Considering the sequences of the RHOD domains fused with SQRs are conserved (Fig. 8 & S14), they may also modulate the activity of the fused SQRs.

Genes coding for dissociated rhodaneses is quite common in the *sqr* and *pdo* gene clusters (Table S6). They are expected to play a role during sulfide oxidation by SQR and PDO, and the human mitochondrial rhodanese TSTD1 is speculated to link the activity of SQR and PDO [12]. Our results show that dDUF442 and several *E. coli* rhodaneses enhance the PDO_{Cp} activities (Fig. 5). This finding is similar to that of the RHOD domains fused with PDOs. Both the PDOs from *Staphylococcus aureus* and *Burkholderia phytofirmans* have a C-terminal RHOD domain, whose loss would severely weaken the PDO activities [15,34].

There are *sqr-pdo* gene clusters that do not contain RHOD. Our results indicate that *E. coli* MG1655 has several dissociated RHODs and their activity is sufficient to support sulfide oxidation by cloned SQR and PDO, preventing the accumulation of cellular sulfane sulfur (Fig. S4). Since rhodanese genes are widely present in bacterial genomes [17], the bacteria should possess other rhodaneses to work with SQR and PDO if a rhodanese gene is not next to *sqr* and *pdo* genes. Hence, the role of RHOD in keeping cellular redox homeostasis could be a prevalent mode during the sulfide oxidation process.

In summary, genes coding for fused RHOD domains or dissociated RHODs is widely present in bacterial *sqr* and *pdo* gene clusters (Table S6). The function of RHOD during sulfide oxidation by SQR and PDO is to prevent the accumulation of cellular sulfane sulfur (Fig. 9). The fDUF442 domain of SQR_{Cp} modulates the SQR activity to prevent the production of excessive sulfane sulfur (Fig. 9A), and dissociated RHODs enhance the PDO activity to expedite the consumption of sulfane sulfur (Fig. 9B). The accumulation of cellular sulfane sulfur causes GSH oxidation into GSSG, an indication of disulfide stress. Thus, RHODs and RHOD domains prevent the accumulation of cellular sulfane sulfur to prevent disulfide stress during sulfide oxidation.

Funding

The work was financially supported by grants from the National Natural Science Foundation of China (91951202, 31870085, 31961133015, 31870097).

Data availability

All data are reported in the main text or Supplementary Data.

Declaration of interests

The authors declare that they have no known competing financial interests or personal relationships that could have appeared to influence the work reported in this paper.

Appendix A. Supplementary data

Supplementary data to this article can be found online at https://doi.org/10.1016/j.redox.2022.102345.

References

[1] Kenneth R. Olson, K.D. Straub, The role of hydrogen sulfide in evolution and the evolution of hydrogen sulfide in metabolism and signaling, Physiology 31 (2016) 60–72.
[2] Brennah Murphy, Resham Bhattacharya, M. Priyabrata, Hydrogen sulfide signaling in mitochondria and disease, Faseb. J. 33 (2019) 13098–13125.
[3] A.K. Mustafa, M.M. Gadalla, N. Sen, S. Kim, W. Mu, S.K. Gazi, R.K. Barrow, G. Yang, R. Wang, S.H. Snyder, H_2S signals through protein S-sulfhydration, Sci. Signal. 2 (2009) ra72.
[4] Aroca Angeles, Gotor Cecilia, Romero Luis, Hydrogen sulfide signaling in plants: emerging roles of protein persulfidation, Front. Plant Sci. 9 (2018) 1369.
[5] Angeles, Aroca, Cecilia, Gotor, Luis, C. Romero, Hydrogen sulfide sensing through reactive sulfur species (RSS) and nitroxyl (HNO) in Enterococcus faecalis, ACS Chem. Biol. 13 (2018) 1610–1620.
[6] C. Szabo, C. Ransy, K. Modis, M. Andriamihaja, B. Murghes, C. Coletta, G. Olah, K. Yanagi, F. Bouillaud, Regulation of mitochondrial bioenergetic function by hydrogen sulfide. Part I. Biochemical and physiological mechanisms, Br. J. Pharmacol. 171 (2014) 2099–2122.
[7] P. Nicholls, Inhibition of cytochrome c oxidase by sulphide, Biochem. Soc. Trans. 3 (1975) 316–319.
[8] C. Zheng, S. Guo, W.G. Tennant, P.K. Pradhan, K.A. Black, P.C.D. Santos, The thioredoxin system reduces protein persulfide intermediates formed during the synthesis of thio-cofactors in Bacillus subtilis, Biochemistry 58 (2019) 1892–1904.
[9] Y. Xia, C. Lu, N. Hou, Y. Xin, J. Liu, H. Liu, L. Xun, Sulfide production and oxidation by heterotrophic bacteria under aerobic conditions, ISME J. 11 (2017) 2754.
[10] C.J. Lu, Y.Z. Xia, D.X. Liu, R. Zhao, R. Gao, H.L. Liu, L.Y. Xun, Cupriavidus necator H16 Uses flavocytochrome c sulfide dehydrogenase to oxidize self-produced and added sulfide, Appl. Environ. Microbiol. 83 (2017) 14.
[11] Y. Xin, H. Liu, F. Cui, H. Liu, L. Xun, Recombinant Escherichia coli with sulfide: quinone oxidoreductase and persulfide dioxygenase rapidly oxidises sulfide to sulfite and thiosulfate via a new pathway, Environ. Microbiol. 18 (2016) 5123–5136.
[12] S.L. Melideo, M.R. Jackson, M.S. Jorns, Biosynthesis of a central intermediate in hydrogen sulfide metabolism by a novel human sulfurtransferase and its yeast ortholog, Biochemistry 53 (2014) 4739–4753.

[13] M. Libiad, P.K. Yadav, V. Vitvitsky, M.V. Martinov, R. Banerjee, Organization of the human mitochondrial hydrogen sulfide oxidation pathway, J. Biol. Chem. 289 (2014) 30901–30910.
[14] K.A. Higgins, H. Peng, J.L. Luebke, F.J. Chang, D.P. Giedroc, Conformational analysis and chemical reactivity of the multidomain sulfurtransferase, Staphylococcus aureus CstA, Biochemistry 54 (2015) 2385–2398.
[15] J. Shen, M.E. Keithly, R.N. Armstrong, K.A. Higgins, K.A. Edmonds, D.P. Giedroc, Staphylococcus aureus CstB is a novel multidomain persulfide dioxygenase-sulfurtransferase involved in hydrogen sulfide detoxification, Biochemistry 54 (2015) 4542–4554.
[16] H. Liu, Y. Xin, L. Xun, Distribution, diversity, and activities of sulfur dioxygenases in heterotrophic bacteria, Appl. Environ. Microbiol. 80 (2014) 1799–1806.
[17] D. Bordo, P. Bork, The rhodanese/Cdc25 phosphatase superfamily, EMBO Rep. 3 (2002) 741–746.
[18] W.K. Ray, G. Zeng, M.B. Potters, A.M. Mansuri, T.J. Larson, Characterization of a 12-Kilodalton rhodanese encoded byglpE of Escherichia coli and its interaction with thioredoxin, J. Bacteriol. 182 (2000) 2277–2284.
[19] J.H. Ploegman, G. Drent, K.H. Kalk, W.G. Hol, R.L. Heinrikson, P. Keim, L. Weng, J. Russell, The covalent and tertiary structure of bovine liver rhodanese, Nature 273 (1978) 124–129.
[20] F. Cartini, W. Remelli, P.C. Dos Santos, J. Papenbrock, S. Pagani, F. Forlani, Mobilization of sulfane sulfur from cysteine desulfurases to the Azotobacter vinelandii sulfurtransferase RhdA, Amino acids 41 (2011) 141–150.
[21] N.L. Hepowit, J.A. Maupin-Furlow, Rhodanese-like domain protein UbaC and its role in ubiquitin-like protein modification and sulfur mobilization in Archaea, J. Bacteriol. (2019). JB. 00254-00219.
[22] P.M. Palenchar, C.J. Buck, H. Cheng, T.J. Larson, E.G. Mueller, Evidence that ThiI, an enzyme shared between thiamin and 4-thiouridine biosynthesis, may be a sulfurtransferase that proceeds through a persulfide intermediate, J. Biol. Chem. 275 (2000) 8283–8286.
[23] R. Cipollone, P. Ascenzi, P. Visca, Common themes and variations in the rhodanese superfamily, IUBMB Life 59 (2007) 51–59.
[24] Y. Mikami, N. Shibuya, Y. Kimura, N. Nagahara, Y. Ogasawara, H. Kimura, Thioredoxin and dihydrolipoic acid are required for 3-mercaptopyruvate sulfurtransferase to produce hydrogen sulfide, Biochem. J. 439 (2011) 479–485.
[25] A. Bilska-Wilkosz, M. Iciek, D. Kowalczyk-Pachel, M. Gorny, M. Sokolowska-Jezewicz, L. Wlodek, Lipoic acid as a possible pharmacological source of hydrogen sulfide/sulfane sulfur, Molecules 22 (2017) 11.
[26] M. Wrobel, B. Papla, Rhodanese activity and total sulfur content in frog and mouse liver, Folia Histochem. Cytobiol. 38 (2000) 11–17.
[27] M.D. Wolfe, F. Ahmed, G.M. Lacourciere, C.T. Lauhon, T.C. Stadtman, T.J. Larson, Functional diversity of the rhodanese homology domain - the Escherichia coli ybbB gene encodes a selenophosphate-dependent tRNA 2-selenouridine synthase, J. Biol. Chem. 279 (2004) 1801–1809.
[28] N.C. Martinez-Gomez, L.D. Palmer, E. Vivas, P.L. Roach, D.M. Downs, The rhodanese domain of ThiI is both necessary and sufficient for synthesis of the thiazole moiety of thiamine in Salmonella enterica, J. Bacteriol. 193 (2011) 4582–4587.
[29] S. Leimkuhler, M. Buhning, L. Beilschmidt, Shared sulfur mobilization routes for tRNA thiolation and molybdenum cofactor biosynthesis in prokaryotes and eukaryotes, Biomolecules 7 (2017) 5.
[30] N. Nagahara, A. Katayama, Post-translational regulation of mercaptopyruvate sulfurtransferase via a low redox potential cysteine-sulfenate in the maintenance of redox homeostasis, J. Biol. Chem. 280 (2005) 34569–34576.
[31] W. Remelli, A. Cereda, J. Papenbrock, F. Forlani, S. Pagani, The rhodanese RhdA helps Azotobacter vinelandii in maintaining cellular redox balance, Biol. Chem. 391 (2010) 777–784.
[32] A. Steiner, C. Busching, H. Vogel, U. Wittstock, Molecular identification and characterization of rhodaneses from the insect herbivore Pieris rapae, Sci. Rep. 8 (2018) 10819, 10819.
[33] T. Tang, C. Ji, Z. Yang, F. Liu, S. Xie, Involvement of the Macrobrachium nipponense rhodanese homologue 2, MnRDH2 in innate immunity and antioxidant defense, Fish Shellfish Immunol. 70 (2017) 327–334.
[34] N. Motl, M.A. Skiba, O. Kabil, J.L. Smith, R. Banerjee, Structural and biochemical analyses indicate that a bacterial persulfide dioxygenase—rhodanese fusion protein functions in sulfur assimilation, J. Biol. Chem. 292 (2017) 14026–14038.
[35] H. Cheng, J.L. Donahue, S.E. Battle, W.K. Ray, T.J. Larson, Biochemical and genetic characterization of PspE and GlpE, two single- domain sulfurtransferases of Escherichia coli, Open Microbiol. J. 2 (2008) 18–28.
[36] Y. Xia, K. Li, J. Li, T. Wang, L. Gu, L. Xun, T5 exonuclease-dependent assembly offers a low-cost method for efficient cloning and site-directed mutagenesis, Nucleic Acids Res. 47 (2018), e15 e15.
[37] K.A. Datsenko, B.L. Wanner, One-step inactivation of chromosomal genes in Escherichia coli K-12 using PCR products, Proc. Natl. Acad. Sci. Unit. States Am. 97 (2000) 6640–6645.
[38] M. Li, J. Wang, Y. Geng, Y. Li, Q. Qi, A strategy of gene overexpression based on tandem repetitive promoters in Escherichia coli, Microb. Cell Factories 11 (2012) 19, 19.
[39] B. Sörbo, Rhodanese, 1955.
[40] A. Argyrou, J.S. Blanchard, Flavoprotein disulfide reductases: advances in chemistry and function, Prog. Nucleic Acid Res. Mol. Biol. 78 (2004) 89–142.
[41] R. Michael, Jackson, L. Scott, Marilyn Melideo, Jorns Schuman, Human sulfide: quinone oxidoreductase catalyzes the first step in hydrogen sulfide metabolism and produces a sulfane sulfur metabolite, Biochemistry 51 (2012) 6804–6815.
[42] R. Gao, H. Liu, L. Xun, Cytoplasmic localization of sulfide:quinone oxidoreductase and persulfide dioxygenase of Cupriavidus pinatubonensis JMP134, Appl. Environ. Microbiol. 83 (2017).
[43] Y. Xin, R. Gao, F. Cui, C. Lü, L. Xun, The heterotrophic bacterium Cupriavidus pinatubonensis JMP134 oxidizes sulfide to sulfate with thiosulfate as a key intermediate, Appl. Environ. Microbiol. 86 (2020), e01835, 01820.
[44] J.M. Visser, L.A. Robertson, H. W, J.G.A. Kuenen, Sulfur production by obligately chemolithoautotrophic thiobacillus species, Appl. Environ. Microbiol. 63 (1997) 2300.
[45] J.R. Biggs, A.S. Kraft, The role of the Smad3 protein in phorbol ester-induced promoter expression, J. Biol. Chem. 274 (1999) 36987–36994.
[46] R. Moest, Hydrogen sulfide determination by the methylene blue method, Anal. Chem. 47 (1975) 1204–1205.
[47] M. Ran, T. Wang, M. Shao, Z. Chen, H. Liu, Y. Xia, L. Xun, Sensitive method for reliable quantification of sulfane sulfur in biological samples, Anal. Chem. 91 (2019) 11981–11986.
[48] F. Aslund, M. Zheng, J. Beckwith, G. Storz, Regulation of the OxyR transcription factor by hydrogen peroxide and the cellular thiol-disulfide status, Proc. Natl. Acad. Sci. Unit. States Am. 96 (1999) 6161–6165.
[49] M.E. Anderson, Determination of glutathione and glutathione disulfide in biological samples, in: Methods in Enzymology, vol. 113, Elsevier, 1985, pp. 548–555.
[50] H. McWilliam, W.Z. Li, M. Uludag, S. Squizzato, Y.M. Park, N. Buso, A.P. Cowley, R. Lopez, Analysis tool web services from the EMBL-EBI, Nucleic Acids Res. 41 (2013) W597–W600.
[51] S.-s. Chng, R.J. Dutton, K. Denoncin, D. Vertommen, J. Collet, H. Kadokura, J. Beckwith, Overexpression of the rhodanese PspE, a single cysteine-containing protein, restores disulphide bond formation to an Escherichia coli strain lacking DsbA, Mol. Microbiol. 85 (2012) 996–1006.
[52] A. Sen, J.A. Imlay, How microbes defend themselves from incoming hydrogen peroxide, Front. Immunol. 12 (2021) 667343.
[53] S.A. Sattler, X. Wang, K.M. Lewis, P.J. Dehan, C.M. Park, Y. Xin, H. Liu, M. Xian, L. Xun, C.H. Kang, Characterizations of two bacterial persulfide dioxygenases of the metallo-β-lactamase superfamily, J. Biol. Chem. 290 (2015) 18914–18923.
[54] T.M. Hildebrandt, M.K. Grieshaber, Three enzymatic activities catalyze the oxidation of sulfide to thiosulfate in mammalian and invertebrate mitochondria, FEBS J. 275 (2008) 3352–3361.
[55] I. Sato, K. Shimatani, K. Fujita, T. Abe, M. Shimizu, T. Fujii, T. Hoshino, N. J. Takaya, Glutathione reductase/glutathione is responsible for cytotoxic elemental sulfur tolerance via polysulfide shuttle in fungi, J. Biol. Chem. 286 (2011) 20283–20291.
[56] N. Hou, Z. Yan, K. Fan, H. Li, R. Zhao, Y. Xia, L. Xun, H. Liu, OxyR senses sulfane sulfur and activates the genes for its removal in Escherichia coli, Redox Biol. 26 (2019), 101293.
[57] N.S. Kosower, E.M. Kosower, B. Wertheim, W.S. Correa, Diamide, a new reagent for the intracellular oxidation of glutathione to the disulfide, Biochem. Biophys. Res. Commun. 37 (1969) 593–596.
[58] R. Wax, E. Rosenberg, N.S. Kosower, E.M. Kosower, Effect of the thiol-oxidizing agent diamide on the growth of Escherichia coli, J. Bacteriol. 101 (1970) 1092–1093.
[59] M. Hillion, H. Antelmann, Thiol-based redox switches in prokaryotes, Biol. Chem. 396 (2015) 415–444.
[60] N. Dickerhof, V. Isles, P. Pattemore, M.B. Hampton, A.J. Kettle, Exposure of Pseudomonas aeruginosa to bactericidal hypochlorous acid during neutrophil phagocytosis is compromised in cystic fibrosis, J. Biol. Chem. 294 (2019) 13502–13514.
[61] X. Li, J.A. Imlay, Improved measurements of scant hydrogen peroxide enable experiments that define its threshold of toxicity for Escherichia coli, Free Radic. Biol. Med. 120 (2018) 217–227.
[62] S. Korshunov, K.R.C. Imlay, J.A. Imlay, Cystine import is a valuable but risky process whose hazards Escherichia coli minimizes by inducing a cysteine exporter, Mol. Microbiol. 113 (2020) 22–39.
[63] A.P. Landry, S. Moon, H. Kim, P.K. Yadav, A. Guha, U.S. Cho, R. Banerjee, A catalytic trisulfide in human sulfide quinone oxidoreductase catalyzes coenzyme A persulfide synthesis and inhibits butyrate oxidation, Cell Chem. Biol. 26 (2019) 1515–1525.
[64] A.P. Landry, D.P. Ballou, R. Banerjee, Modulation of catalytic promiscuity during hydrogen sulfide oxidation, ACS Chem. Biol. 13 (2018) 1651–1658.